

# Journal Pre-proof

Synthesis of Eu(III) fabricated spinel ferrite based surface modified hybrid nanocomposite: Study of catalytic activity towards the facile synthesis of tetrahydrobenzo[*b*]pyrans

Taiebeh Tamoradi, Bikash Karmakar, Maryam Kamalzare, Mohammad Bayat, Afsaneh Taheri Kal-Koshvndi, Ali Maleki

PII: S0022-2860(20)30923-6

DOI: <https://doi.org/10.1016/j.molstruc.2020.128598>

Reference: MOLSTR 128598

To appear in: *Journal of Molecular Structure*

Received Date: 4 May 2020

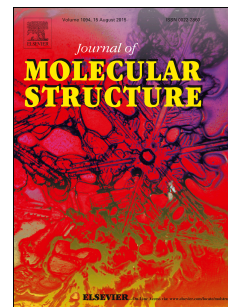
Revised Date: 30 May 2020

Accepted Date: 2 June 2020

Please cite this article as: T. Tamoradi, B. Karmakar, M. Kamalzare, M. Bayat, A.T. Kal-Koshvndi, A. Maleki, Synthesis of Eu(III) fabricated spinel ferrite based surface modified hybrid nanocomposite: Study of catalytic activity towards the facile synthesis of tetrahydrobenzo[*b*]pyrans, *Journal of Molecular Structure* (2020), doi: <https://doi.org/10.1016/j.molstruc.2020.128598>.

This is a PDF file of an article that has undergone enhancements after acceptance, such as the addition of a cover page and metadata, and formatting for readability, but it is not yet the definitive version of record. This version will undergo additional copyediting, typesetting and review before it is published in its final form, but we are providing this version to give early visibility of the article. Please note that, during the production process, errors may be discovered which could affect the content, and all legal disclaimers that apply to the journal pertain.

© 2020 Published by Elsevier B.V.



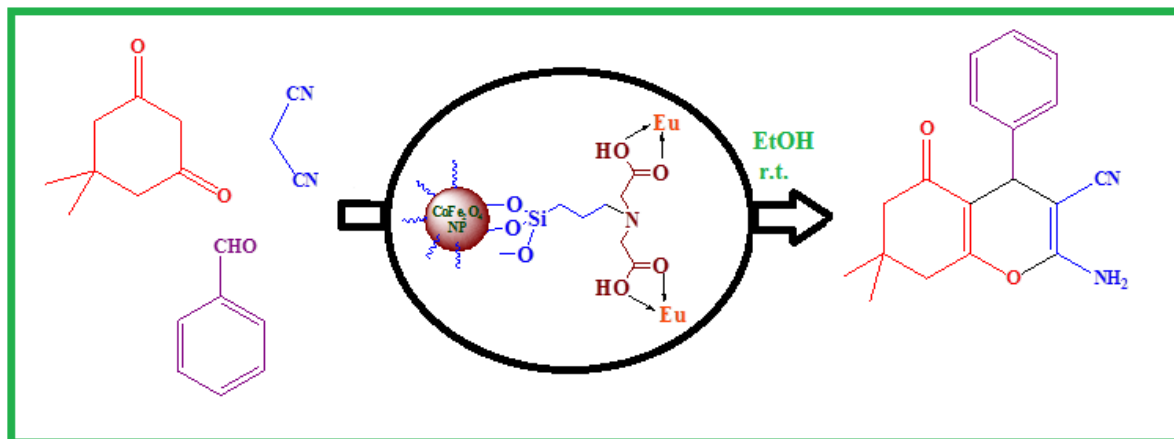
### **Credit author statement**

**Taiebeh Tamoradi:** Conceptualization, Methodology. **Bikash Karmakar:** Writing - Original Draft, Data Curation. **Maryam Kamalzare:** Investigation. **Mohammad Bayat:** Resources. **Afsaneh Taheri Kal-Koshvandi:** Methodology, Writing- Reviewing and Editing, Supervision.

Journal Pre-proof

**Synthesis of Eu(III) fabricated spinel ferrite based surface modified hybrid nanocomposite : Study of catalytic activity towards the facile synthesis of tetrahydrobenzo[b]pyrans**

Taiebeh Tamoradi, Bikash Karmakar, Maryam Kamalzare, Mohammad Bayat, Afsaneh Taheri Kal-Koshvandi,\* Ali Maleki



## Synthesis of Eu(III) fabricated spinel ferrite based surface modified hybrid nanocomposite : Study of catalytic activity towards the facile synthesis of tetrahydrobenzo[*b*]pyrans

Taiebeh Tamoradi,<sup>b</sup> Bikash Karmakar,<sup>c</sup> Maryam Kamalzare,<sup>a,d</sup> Mohammad Bayat,<sup>d</sup> Afsaneh Taheri Kal-Koshvandi,<sup>a,\*</sup> Ali Maleki<sup>a</sup>

<sup>a</sup>Catalysts and Organic Synthesis Research Laboratory, Department of Chemistry, Iran University of Science and Technology, Tehran, 16846-13114, Iran

<sup>b</sup>Department of Chemistry, Islamic Azad University, Izeh, Iran

<sup>c</sup>Department of Chemistry, Gobardanga Hindu College, India

<sup>d</sup>Department of Chemistry, Faculty of Science, Imam Khomeini International University, Qazvin, Iran

\*Corresponding author e-mail: [afsaneh.taheri96@yahoo.com](mailto:afsaneh.taheri96@yahoo.com); Tel: +98-9904506849

### Abstract

The present work demonstrates a modified protocol for the synthesis of Europium (Eu) anchored iminodiacetic acid functionalized silica modified core-shell  $\text{CoFe}_2\text{O}_4$  magnetic nanoparticles. This is the first report of Eu immobilized nanocomposite in the synthesis of biologically active organic compounds. The structural and physicochemical characteristics of the material were evaluated using different analytical techniques such as Fourier transformed infrared spectroscopy (FT-IR), Field Emission Scanning Electron Microscopy (FESEM), Energy Dispersive X-ray Spectroscopy (EDX), X-ray Elemental Mapping (WDX) and X-ray Diffraction study (XRD). The Eu(III)/IDA/CPTS/ $\text{CoFe}_2\text{O}_4$  nanocomposite was catalytically investigated in the multicomponent green synthesis of diverse substituted tetrahydrobenzo[*b*]pyrans by coupling dimedone, malononitrile and a wide range of aromatic aldehydes. The magnetically retrievable catalyst was stable enough to be reused up to six consecutive times in the reaction without considerable loss in activity.

**Keywords:** Magnetic NP; Iminodiacetic acid; Eu(III) catalysis; Multicomponent reaction (MCR); Tetrahydrobenzo[*b*]pyran; Reusability.

## 1. Introduction

In current material science the synthesis and applications of advanced functional nanomaterials has garnered high attention due to their distinctive characteristics like site selective chemical properties, tunable size and shape dependent physical properties, large surface to volume ratio, exceptional thermal and mechanical stability etc<sup>1-3</sup>. In continuation to that trend, the use of magnetic nanoparticles in heterogeneous green catalysis has become highly significant based on their easy recovery from the reaction solutions and facile recycling by an external magnet, cost-effectiveness and bio-compatibility.<sup>4,5</sup> In addition, they acquire high surface to volume ratio, enhanced reactivity due to large number of active sites, high selectivity and thermal stability.<sup>6</sup> Due to such implications, magnetic nanoparticles (MNPs) have been greatly used in many catalytic reactions such as, oxidation,<sup>7</sup> C-C and C-heteroatom coupling,<sup>8,9</sup> condensation,<sup>10</sup> cycloaddition,<sup>11</sup> photocatalysis, drug delivery<sup>12</sup> and sensors<sup>13</sup>.

Among the different magnetic nanomaterials, transition metal ferrites are of special priority due to their unique electronic, catalytic and magnetic behaviors.<sup>5</sup> The spinel ferrites possess general formula  $MFe_2O_4$  ( $M = Mn^{2+}, Fe^{2+}, Co^{2+}, Ni^{2+}, Cu^{2+}$  and  $Zn^{2+}$ ), commonly known as multiferrites. Owing to their special structural designs, they are more stable and bear higher paramagnetism than bare  $Fe_3O_4$ .<sup>5</sup> In particular,  $CoFe_2O_4$  acquires special attention due to its applications in different fields like sensing, catalysis, electronics, magnetism and medicinal therapeutics.<sup>14</sup> Moreover, the large number of surface hydroxyl groups present in their periphery facilitates them towards surface modifications with suitable organic ligands.<sup>15-16</sup> These organic linkers can be exploited to introduce a secondary layer of metal species as active constituent in catalysis.<sup>5</sup> In this article, we actually have adopted this very concept and introduced diminodiacetic acid (IDA)

as the organic linker. IDA is a bis-glycine analog and a very good chelating ligand binding the incoming metal in (1 : 2) ratio (Scheme 1).

4*H*-pyran derivatives are important class of heterocyclic motifs having tremendous biological applications.<sup>17</sup> Specifically, tetrahydrobenzo[*b*]pyrans have been reported to have plethora of pharmacological activities.<sup>18</sup> They are important antitumor, anti-cancer,<sup>19</sup> antiviral, anti-allergenic, anti-ancaphylactic, anti-coagulant, antileishmanial, spasmolytic and diuretic compounds<sup>20</sup>, antioxidant, antibacterial,<sup>21</sup> and antifungal<sup>22</sup> compounds. They also have been accounted for cognitive enhancers in the treatment of various neurodegenerative diseases, including Alzheimer's disease, Huntington's disease, Down's syndrome, AIDS-associated dementia,<sup>23</sup> Parkinson's disease,<sup>24</sup> and treatment of schizophrenia.<sup>25</sup> Some of the significant bioactive benzo[*b*]pyran derivatives have been shown in Fig 1.

Considering all these implications, synthesis of the scaffold has been of great interest and thereby a number of synthetic methodologies have been explored by several groups.<sup>26-28</sup> Keeping in view of sustainable chemistry, multicomponent reaction (MCR)<sup>29,30</sup> has been the most promising protocol for the synthesis of such molecular hybrid. Thereby, the target molecule could be built up by assembling dimedone, malononitrile and aldehydes. Different catalysts have been reported for that procedure, like SiO<sub>2</sub> NPs,<sup>31</sup> Bi<sub>2</sub>WO<sub>6</sub> NPs,<sup>32</sup> Ni<sub>0.5</sub>Zn<sub>0.5</sub>Fe<sub>2</sub>O<sub>4</sub>@HA-PRS NPs,<sup>33</sup> caffeine supported silica,<sup>34</sup> ZnO-β zeolite,<sup>35</sup> etc. Nonetheless, keeping in mind of their own intrinsic worth, there is always scope of method development for the synthesis following the pathway of sustainable green catalysis. Thereby, as part of our ongoing research based on the multicomponent reaction,<sup>36-39</sup> we would like to report the Eu (Europium) anchored iminodiacetic acid (IDA) ligand functionalized CoFe<sub>2</sub>O<sub>4</sub> nanoparticles as a magnetically isolable nanocatalyst towards the multicomponent synthesis of 2-amino-3-cyano tetrahydrobenzo[*b*]pyrans for the

first time (Scheme 1 and 2). All the reactions were performed in ethanolic media at room temperature and excellent yields were obtained in short reaction times.

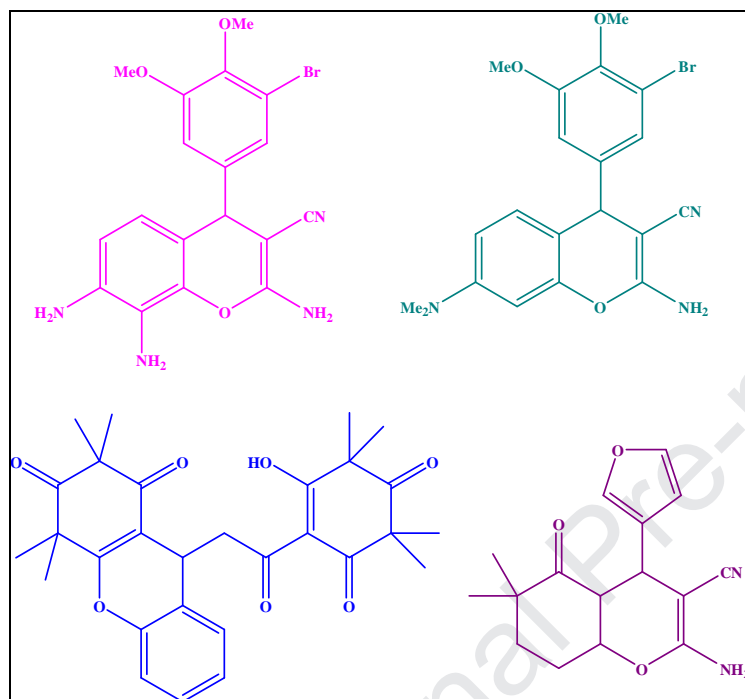
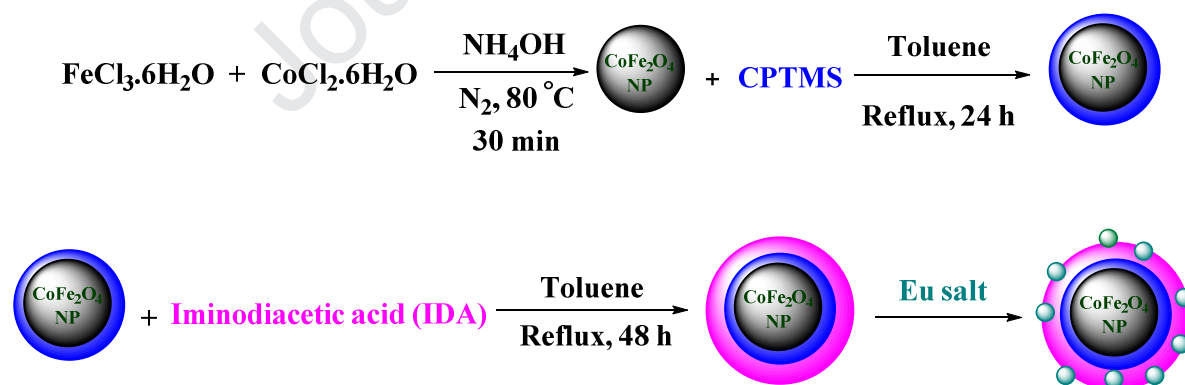
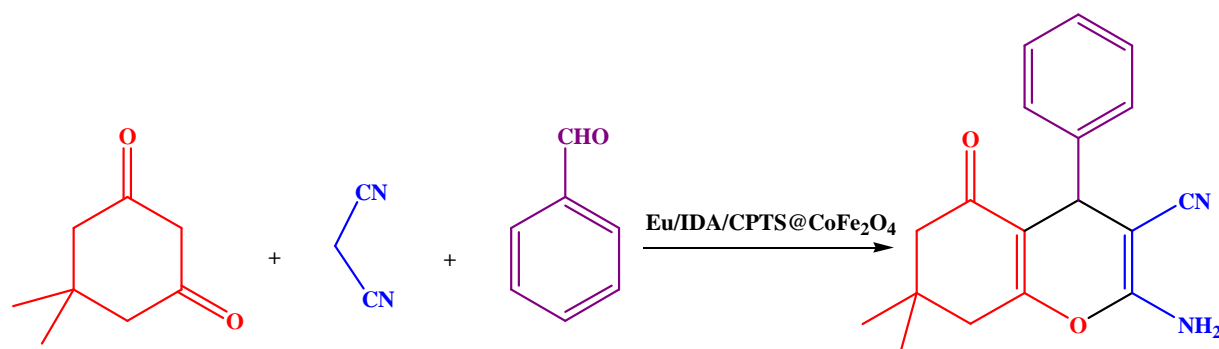


**Fig.1.** Examples of some bioactive molecules containing benzo[*b*]pyran scaffold



**Scheme 1.** Synthesis of Eu@MNPs nanocomposite



**Scheme 2.** Eu nanocomposite catalyzed multicomponent synthesis of tetrahydrobenzo[*b*]pyrans

## 2. Experimental

### 2.1 Materials and instrumentations

The chemicals necessary for the synthesis of catalyst, such as, FeCl<sub>3</sub>·6H<sub>2</sub>O, CoCl<sub>2</sub>·6H<sub>2</sub>O, 3-chloropropyl trimethoxysilane (CPTMS), iminodiacetic acid (IDA) and Eu(NO<sub>3</sub>)<sub>3</sub> were purchased from Sigma-Aldrich. The chemicals required for organic synthesis and the essential solvents were purchased from Merck. All the reagents were used as such without further purification. FT-IR analysis (KBr disc) was done using a VRTEX 70 model BRUKER FT-IR spectrophotometer. The particle morphology, shape, size and atomic mapping of the material were studied using a FESEM-TESCAN MIRA3 microscope equipped with EDX (TSCAN). In order to analyze the crystallite nature powder XRD was recorded using Co K $\alpha$  radiation ( $\lambda = 1.78897 \text{ \AA}$ ) with an operating voltage of 40 keV and a cathode current of 40 Ma in the scanning range of  $2\theta = 20$  to  $80^\circ$ . Melting points were recorded in an Electrothermal 9100 apparatus.

### 2.2 Synthesis of CoFe<sub>2</sub>O<sub>4</sub> nanoparticles

2.63 g of FeCl<sub>3</sub>·6H<sub>2</sub>O and 1.19 g of CoCl<sub>2</sub>·6H<sub>2</sub>O were dissolved in 50 mL of deionized water under vigorous stirring. 1: 1 aqueous ammonia solution was added to the mixture dropwise and

stirred at 80 °C for 30 min. Immediately the NP formation started as indicated by blackening of the solution. The products were isolated using a magnet and subsequently washed several times with deionized water followed by ethanol. Finally they were dried at 60 °C for overnight.

### *2.3 Synthesis of CPTS functionalized CoFe<sub>2</sub>O<sub>4</sub> nanoparticles (CPTS@CoFe<sub>2</sub>O<sub>4</sub>)*

For surface modification, 1.0 g of the CoFe<sub>2</sub>O<sub>4</sub> NP was suspended in 30 mL anhydrous toluene and 1.5 mmol of 3-CPTES was added dropwise. The resulting mixture was refluxed for 24 h under stirring condition. After completion, the obtained grey product was separated using an external magnet and washed with ethanol for several times. Finally it was dried in oven at 60 °C.

### *2.4 Synthesis of IDA/CPTS@CoFe<sub>2</sub>O<sub>4</sub> nanocomposite*

For the ligand functionalization, 1.0 g of the CPTS@CoFe<sub>2</sub>O<sub>4</sub> composite was dispersed in 30 mL anhydrous toluene and a 10 mL solution of iminodiacetic acid (IDA) (1.5 mmol) ligand in toluene was added dropwise. The resulting mixture was then refluxed for 48 h to have IDA/CPTS@CoFe<sub>2</sub>O<sub>4</sub> nanocomposite. It was again isolated and processed for the next step in previous manner.

### *2.5 Synthesis of Eu@MNPs nanocomposite*

In this final step the IDA/CPTS@CoFe<sub>2</sub>O<sub>4</sub> nanocomposite (1.0 gm) and Eu(NO<sub>3</sub>)<sub>3</sub> (2.5 mmol) were mixed in ethanol (30 ml). The mixture was refluxed for 16 h, filtered, washed thoroughly with ethanol and dried in vacuum to have the Eu@MNPs nanocomposite.

### *2.6 Multicomponent synthesis of 2-amino-4-aryl-3-cyano tetrahydrobenzo[b]pyrans*

In the typical procedure dimedone (1.0 mmol), malononitrile (1.1 mmol) and aryl aldehyde (1.0 mmol) were mixed together in 10 mL ethanol in presence of 0.03 gm catalyst and stirred at room temperature for requisite time period. After completion (checked by TLC), a solid mass appears in the reaction medium. The catalyst was isolated from the reaction flask by using a magnetic stick. The corresponding product, 2-amino-4-aryl-3-cyanotetrahydrobenzo[*b*]pyran was filtered and recrystallized from hot ethanol.

*Spectral data of 2-amino-4-(2-chlorophenyl)-7,7-dimethyl-5-oxo-5,6,7,8-tetrahydro-4H-chromene-3-carbonitrile (4b)*

$^1\text{H}$  NMR (300 MHz, DMSO-*d*6):  $\delta$  = 0.89 (3H, s, CH<sub>3</sub>), 0.99 (3H, s, CH<sub>3</sub>), 1.96 (2H, dd, CH<sub>2</sub>,  $^2J=15.9$  Hz), 2.16 (2H, dd, CH<sub>2</sub>,  $^2J=16.2$  Hz), 4.91 (1H, s, CH), 7.20 (2H, br s, NH<sub>2</sub>), 7.32 (1H, d, Ar,  $^3J=9$  Hz), 7.41 (1H, t, Ar), 7.64 (1H, t, Ar), 7.78 (1H, d, Ar,  $^3J=9$  Hz).  $^{13}\text{C}$  NMR (75 MHz, DMSO-*d*6):  $\delta$  = 27.13 (2CH<sub>3</sub>), 28.75 (C(CH<sub>3</sub>)), 30.38 (CH), 32.30, 50, 56.80 (C(CN)), 112.78, 119.45, 124.18, 128.31, 130.74, 134.03, 139.44, 149.43, 159.66, 163.19 (C-NH<sub>2</sub>), 196.29 (C=O).

*Spectral data of 2-amino-4-(3-methoxyphenyl)-7,7-dimethyl-5-oxo-5,6,7,8-tetrahydro-4H-chromene-3-carbonitrile (4o)*

$^1\text{H}$  NMR (300 MHz, DMSO-*d*6):  $\delta$  = 0.95 (3H, s, CH<sub>3</sub>), 1.02 (3 H, s, CH<sub>3</sub>) 2.07 (2H, dd, CH<sub>2</sub>,  $^2J=15$  Hz), 2.22 (2H, dd, CH<sub>2</sub>,  $^2J=15$  Hz), 3.69 (3H, s, OCH<sub>3</sub>), 4.12 (1H, s, CH), 6.63 (1H, s, Ar), 6.67 (1H, d, Ar,  $^3J=9$  Hz), 6.74 (1H, d, Ar,  $^3J=9$  Hz), 7 (2H, br s, NH<sub>2</sub>), 7.19 (1H, t, Ar).  $^{13}\text{C}$  NMR (75 MHz, DMSO-*d*6): 27.42 (2CH<sub>3</sub>), 28.79 (C(CH<sub>3</sub>)), 32.39, 35.77 (CH), 50.79, 55.45 (OCH<sub>3</sub>), 58.76 (C(CN)), 111.85, 113.19, 113.88, 120.16, 120.56, 130.20, 146.87, 159.28, 159.59 (C-NH<sub>2</sub>), 163.27 (C-OMe), 196.27 (C=O).

### 3. Results and Discussion

#### 3.1 Catalyst characterizations

We successfully synthesized the nanocomposite following post-functionalization approach. The magnetic core NP provides the necessary arrangement for surface modification. The covalently bonded organic molecule, IDA, is a tetradentate ligand and binds the incoming metal (Eu) in 1 : 2 fashion. The nanocomposite so prepared was systematically characterized using various analytical techniques like Fourier Transformed Infrared Spectroscopy (FT-IR), Scanning Electron Microscopy (SEM), Energy Dispersive X-ray Electron Spectroscopy (EDX), Wavelength dispersive X-ray Electron Spectroscopy (WDX) and X-ray diffraction (XRD) studies. Fig. 2 represents a one-plot comparison of FT-IR spectra of bare  $\text{CoFe}_2\text{O}_4$ ,  $\text{CPTS@CoFe}_2\text{O}_4$ ,  $\text{IDA/CPTS@CoFe}_2\text{O}_4$  and  $\text{Eu@MNPs}$  composites. A sharp characteristic peak appeared at around  $590\text{ cm}^{-1}$  is due to strong metal-oxygen absorption in  $\text{CoFe}_2\text{O}_4$  (Fig. 2a). The hydroxyl functionalities (O-H) over the spinel surface are represented by a broad peak at around  $3350\text{--}3400\text{ cm}^{-1}$ . The typical C-H stretching vibrations, representing the chloropropyl functionalized MNP, appears at  $2900\text{ cm}^{-1}$  in Fig. 2b. IDA functionalization is justified by the strong absorption peaks from COOH group at  $1720\text{ cm}^{-1}$  (C=O stretch) and  $1400\text{ cm}^{-1}$  (O-H bend) respectively. O-H stretching frequency from COOH group overlaps with the  $\text{CoFe}_2\text{O}_4$  surface hydroxyl groups. Spectrum of the two nanocomposites,  $\text{IDA/CPTS@CoFe}_2\text{O}_4$  and  $\text{Eu@MNPs}$  (Fig 2c and 2d) looks alike, which implies that the basic skeletons remained intact even after metal grafting at final stage. However, the Eu attachment to the matrix is exhibited in the widening of C=O stretching peak as shown in Fig 2d.

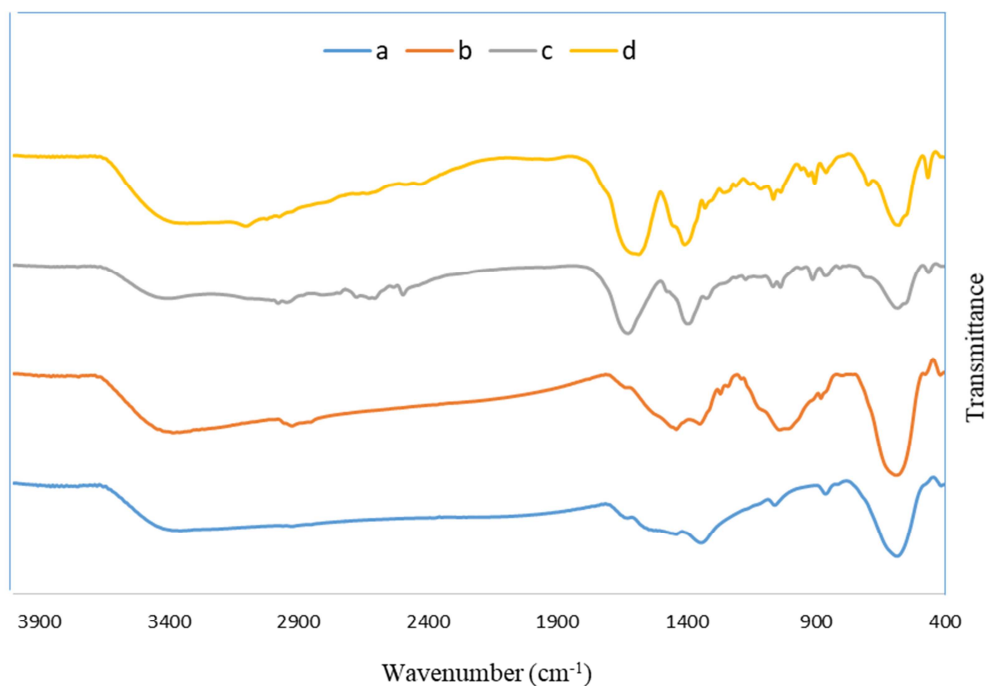


**Fig. 2.** FT-IR spectra of a)  $\text{CoFe}_2\text{O}_4$ , b)  $\text{CPTS@CoFe}_2\text{O}_4$ , c)  $\text{IDA/CPTS@CoFe}_2\text{O}_4$  and d)  $\text{Eu@MNPs}$

The particle morphology and external texture of the synthesized nanocomposite ( $\text{Er/IDA/CPTS@CoFe}_2\text{O}_4$ ) was elucidated by SEM analysis. Fig. 3 represents the images at different magnifications. The material is of fluffy cotton type which might be due to surface modifications. Typically, a bilayer particulate nature is observed from the images. The small grains of particles extended over the whole surface matrix signifies the surface modified active molecules. Higher concentration during sampling is the reason for agglomeration of particles.

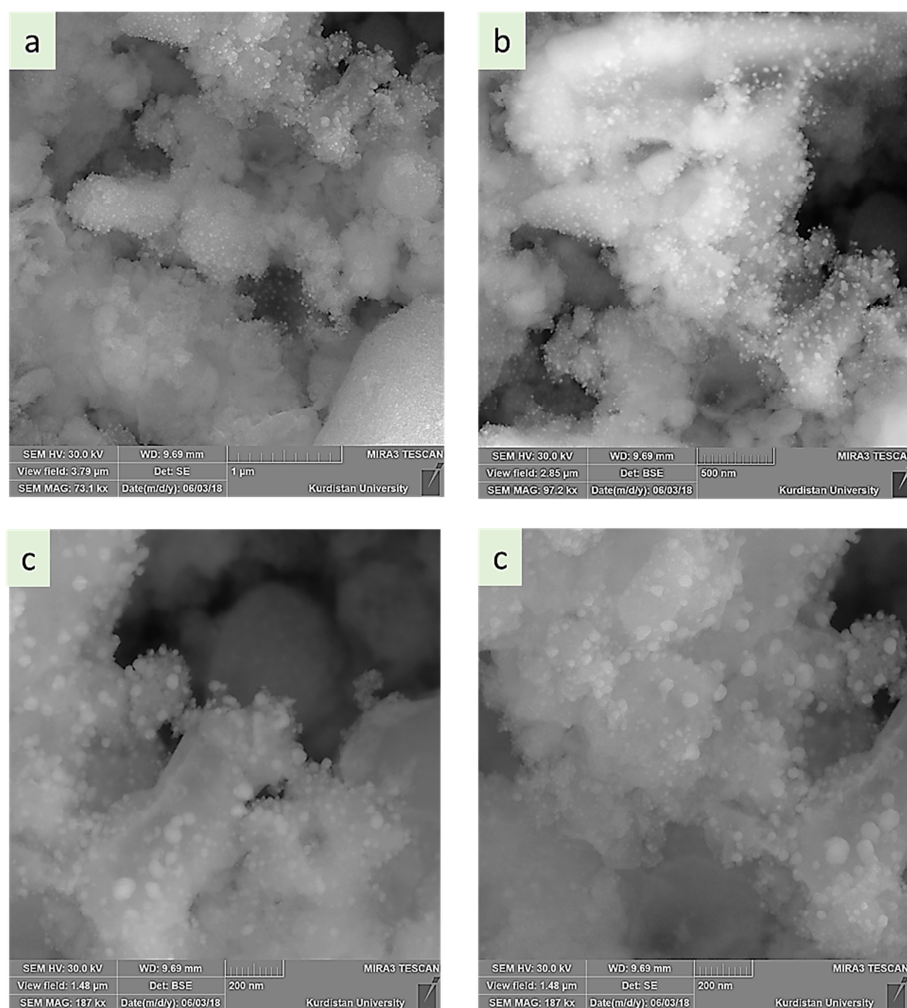


**Fig. 3.** SEM images of Eu@MNPs nanocomposite at different magnifications.

In order to evaluate the elemental composition and structural identity, the Energy-Dispersive X-ray spectroscopy (EDX) of the Eu@MNPs nanocomposite was carried out and the spectrum is presented in Fig. 4. The proposed organic environment around the magnetic core also could be assessed in this analysis. IDA and CPTS attachment are being confirmed by the presence of C, N, O and Si species in the profile. It also exhibits Fe, Co and Eu atoms as a metallic constituent in the nanocomposite.

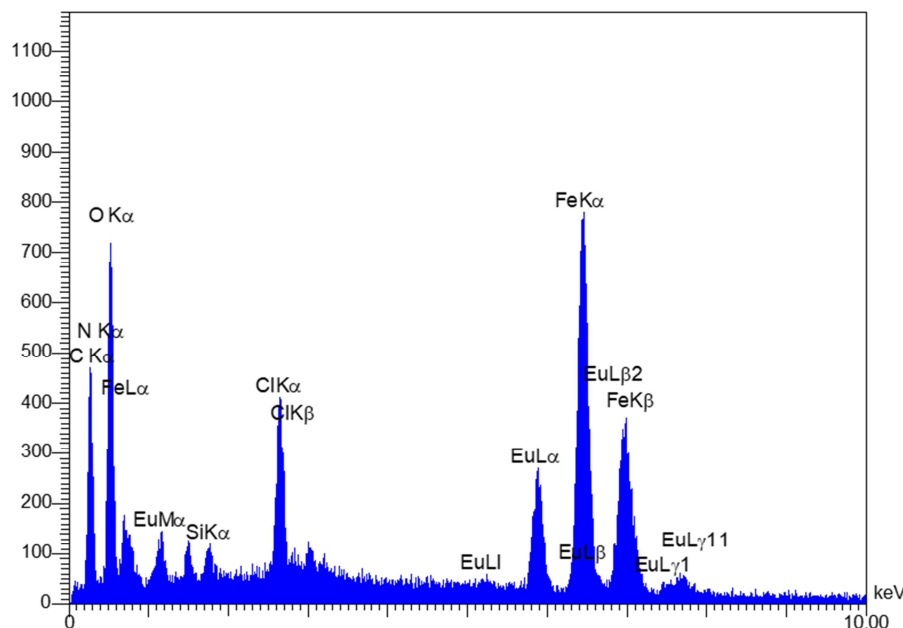


**Fig. 4.**EDX spectrum of the Eu@MNPs nanocomposite

The X-ray atomic mapping or wavelength dispersive X-ray spectroscopy (WDX) is another powerful device to demonstrate the atomic distribution over the catalyst surface with great accuracy. A selected area of SEM image of the composite is scanned with X-ray in the analysis and the result is displayed in Fig. 5. Interestingly, all atoms comprising the material are very well dispersed throughout. It clearly reveals the higher concentration of Fe, Co and O atoms as compared to C, N and Eu. This signifies that the concentrated inner core is made up of  $\text{CoFe}_2\text{O}_4$  and a thin layer of organic functions being bonded to its surface including the Eu at its periphery. The existence of C, N and O atoms additionally confirms the successful attachment of IDA over  $\text{CoFe}_2\text{O}_4$ .

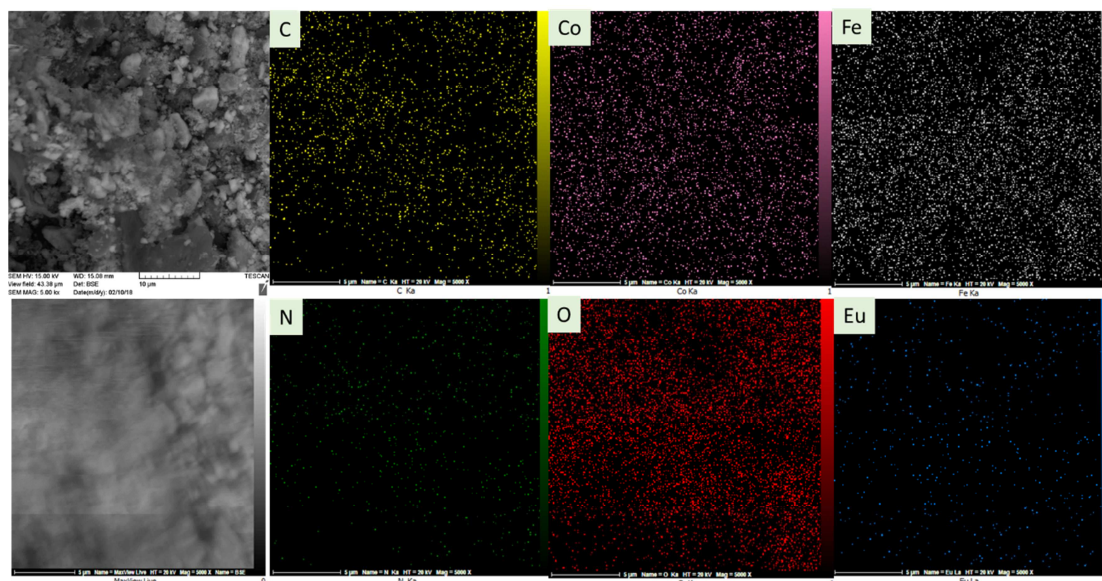


**Fig. 5.** The X-ray atomic mapping of Eu@MNPs nanocatalyst.

To conclude the catalytic characterizations, X-ray diffraction (XRD) study was carried out in order to assess the phase purity and crystallinity of the nanocomposite. It displays a single phase throughout the scanning zone without any phase separation. The diffraction pattern bears a resemblance to that of polycrystalline  $\text{CoFe}_2\text{O}_4$  nanostructure as being authenticated from standard JCPDS values. This evidently substantiates that the basic crystalline phases remains unaltered even after the necessary surface engineering. The peaks appeared in the XRD profile correspond to (2 2 0), (3 1 1), (4 0 0), (4 2 2), (5 1 1) and (4 4 0) crystal planes respectively (Fig. 6).

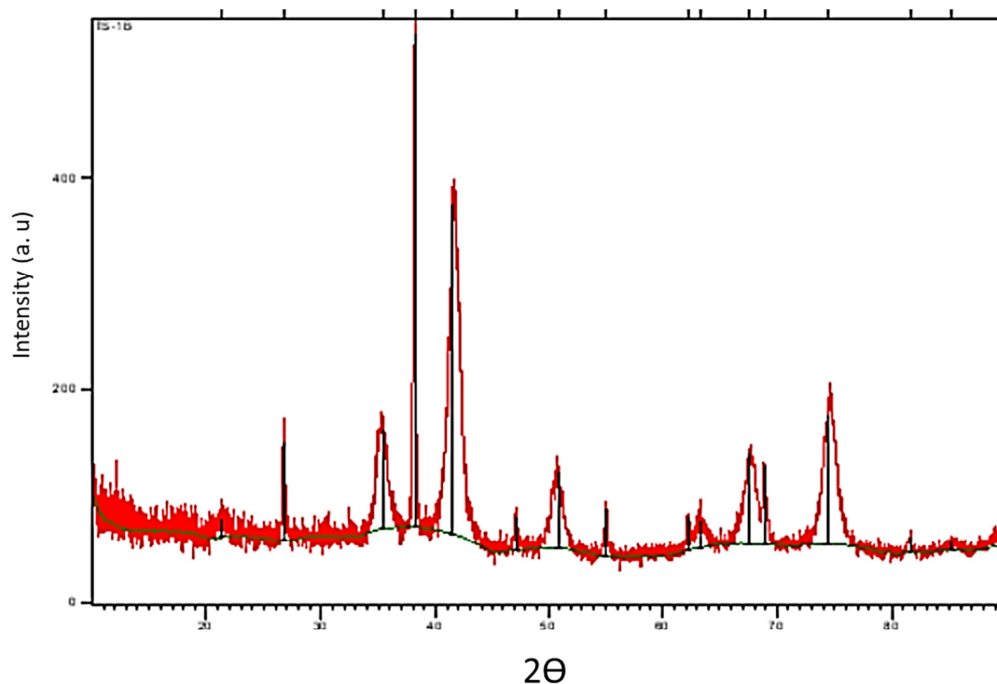


**Fig. 6.** The X-ray diffraction pattern of Eu@MNPs nanocatalyst

### 3.2 Analysis of reaction data

After completion of a rigorous chapter of catalyst synthesis and detailed characterizations, it was the turn to explore the catalytic applications and hence we opted for the synthesis of substituted tetrahydrobenzo[*b*]pyrans by multicomponent coupling over Eu@MNPs nanocatalyst. However, at the outset, optimization of reaction conditions appeared important by selecting a probe reaction between dimedone, malononitrile and 4-chlorobenzaldehyde and then different conditions like solvent, catalyst load and temperature were imposed over it. The results are documented in Table 1.

**Table 1.** Optimization of reaction conditions for the synthesis of 2-amino-4-(4'-chloroaryl)-3-cyanotetrahydrobenzo[*b*]pyrans\*

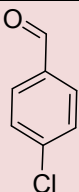
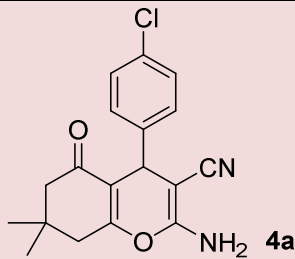
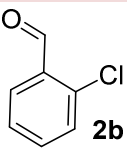
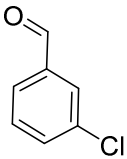
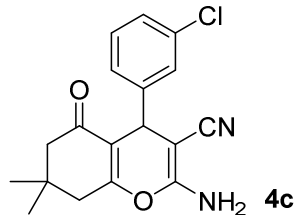
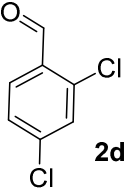
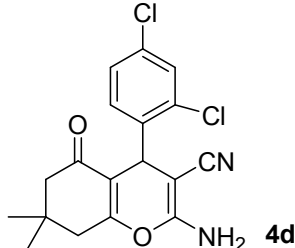
Entry	solvent	temperature	Amount of catalyst(g)	Time (min)	Yield (%)
1	H <sub>2</sub> O	r.t.	—	60	Trace
2	H <sub>2</sub> O	reflux	—	60	30
3	H <sub>2</sub> O	r.t.	0.03	60	70
4	EtOH	r.t.	0.01	60	70
5	EtOH	r.t.	0.02	60	85
6	EtOH	r.t.	0.03	25	96
7	EtOH	r.t.	0.04	25	96
8	CHCl <sub>3</sub>	r.t.	0.03	25	83
9	CH <sub>3</sub> CN	r.t.	0.03	25	91

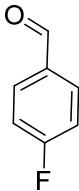
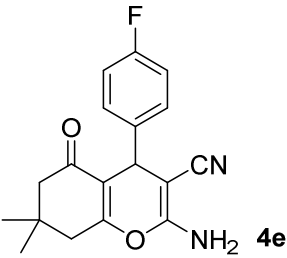
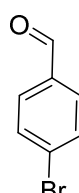
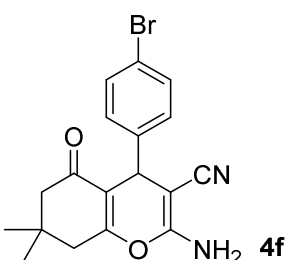
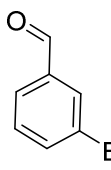
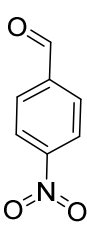
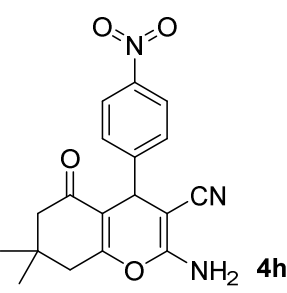
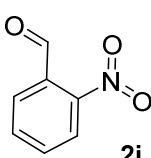
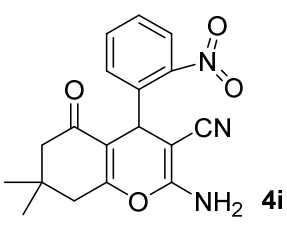
\*Reaction conditions: Dimedone : malononitrile : aldehyde = 1 : 1.1 : 1 (mmol), Eu@MNPs catalyst

Keeping in view of energy conservation, we preferred to carry out the reactions at room temperature. While screening with different solvents like water, ethanol, chloroform and acetonitrile, it was observed that the reaction afforded the best result in ethanol (entry 6-7, Table 1). Only a trace of product was found in the absence of any catalyst (entry 1, Table 1). Even under reflux in water at catalyst-free condition, the yield was not improved. Again, when the reaction was tested with different amount of catalyst load, 0.03 g was found to be the optimum. So, the best condition for the probe reaction was finally set to carry out in ethanol at room temperature in the presence of 0.03 g of catalyst. Now, after having the standard conditions in hand, it was the turn to establish the generality of the conditions and thereby a wide range of aryl aldehydes were reacted with dimedone and malononitrile under the optimized conditions. Different electron withdrawing (F, Cl, Br, NO<sub>2</sub>) and electron donating (OH, OCH<sub>3</sub>, CH<sub>3</sub>, NMe<sub>2</sub>) group substituted aryl aldehydes were well compatible under the reaction conditions and

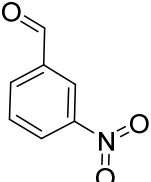
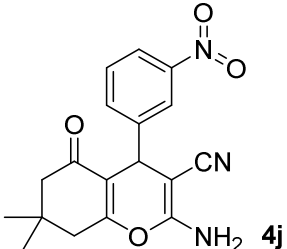
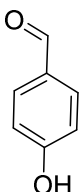
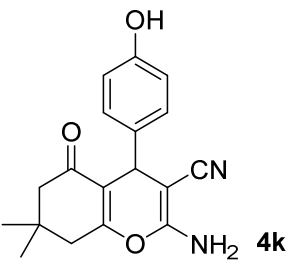
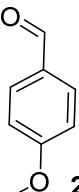
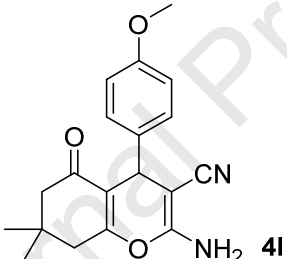
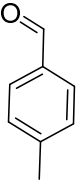
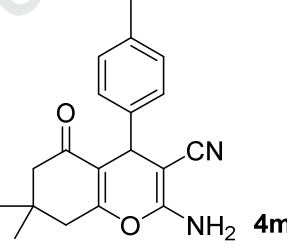
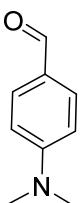
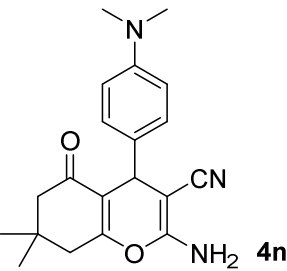
produced excellent yields in short reaction times. The results with isolated yields have been shown in Table 2. All the reactions were found to complete within 25-40 minutes. The products were known and were authenticated by matching with their corresponding melting points.

**Table 2.** Synthesis of diverse substituted tetrahydrobenzo[*b*]pyrans\*

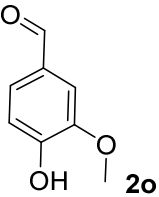
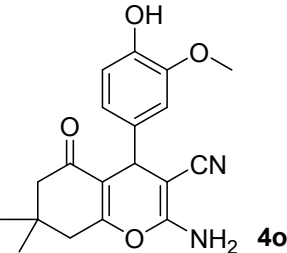
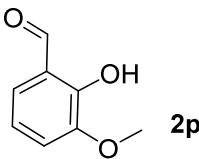
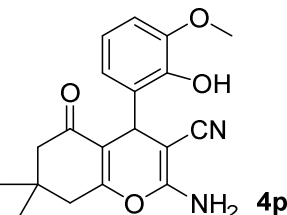
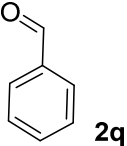
Entry	Aldehyde	Product	Time (min)	Yields (%)	M.p. (Obs) (°C)	M.P. (Lit) (°C)
1	 <b>2a</b>	 <b>4a</b>	25	96	216-219	217-219 (40)
2	 <b>2b</b>	 <b>4b</b>	34	94	215-218	214-216 (41)
3	 <b>2c</b>	 <b>4c</b>	35	92	237-239	234-236 (42)
4	 <b>2d</b>	 <b>4d</b>	25	93	183-184	184-186 (43)

5	 <b>2e</b>	 <b>4e</b>	30	92	186-188	185-189 (44)
6	 <b>2f</b>	 <b>4f</b>	30	91	201-203	205-207 (26)
7	 <b>2g</b>	 <b>4g</b>	35	90	197-199	199-201 (45)
8	 <b>2h</b>	 <b>4h</b>	27	94	153-155	157-159 (46)
9	 <b>2i</b>	 <b>4i</b>	30	91	240-241	236-238 (41)

---

10	 <b>2j</b>	 <b>4j</b>	30	92	218-221	218-219 (47)
11	 <b>2k</b>	 <b>4k</b>	35	88	229-232	223-225 (48)
12	 <b>2l</b>	 <b>4l</b>	40	94	198-200	201-203 (49)
13	 <b>2m</b>	 <b>4m</b>	40	85	213-215	215-217 (50)
14	 <b>2n</b>	 <b>4n</b>	40	84	210-212	213-215 (48)

---

15			30	87	233-236	237-239 (48)
16			40	86	178-180	181-183 (46)
17			35	94	234-236	238-240 (28)

\*Reaction conditions: Dimedone : malononitrile : aldehyde = 1 : 1.1 : 1 (mmol), 0.03 g Eu@MNPs catalyst, EtOH, room temperature stirring.

The plausible mechanistic pathway has been depicted in Fig. 7. Aryl aldehyde and malononitrile being activated over the Eu@MNPs nanocomposite undergoes classical Knoevenagel condensation to generate the intermediate I. Dimedone, the active methylene component then undergoes Michael type addition to I to produce the intermediate II. Subsequently, cyclization occurs via the enolic oxygen affording III. This finally undergoes imine-enamine tautomerisation to afford the final product IV.

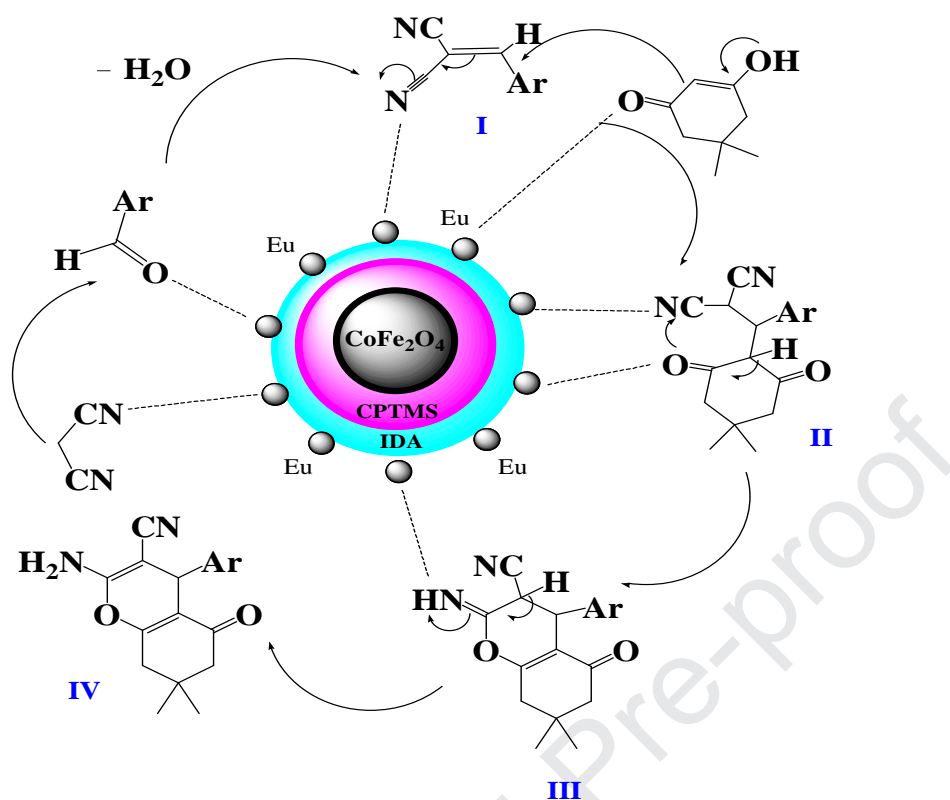


**Fig. 7.** A practical mechanism towards the tetrahydrobenzo[*b*]pyranover  $\text{Eu@MNPs}$  core-shell nanocomposite

### 3.3 Study of reusability

The prime reason to use a magnetic nanocatalyst is the easy isolation from the reaction mixture and its reusability. In view of current green perspectives, this is an important criterion too. Thereby, after completion of a fresh batch of the probe reaction, the  $\text{Eu@MNPs}$  nanocomposite was retrieved using an external bar magnet, washed with solvents and dried. The regenerated catalyst was again used in the further batches of reactions to study its stability and efficiency. Interestingly, it retained its activity for the successive six cycles. The result has been depicted in Fig. 8.

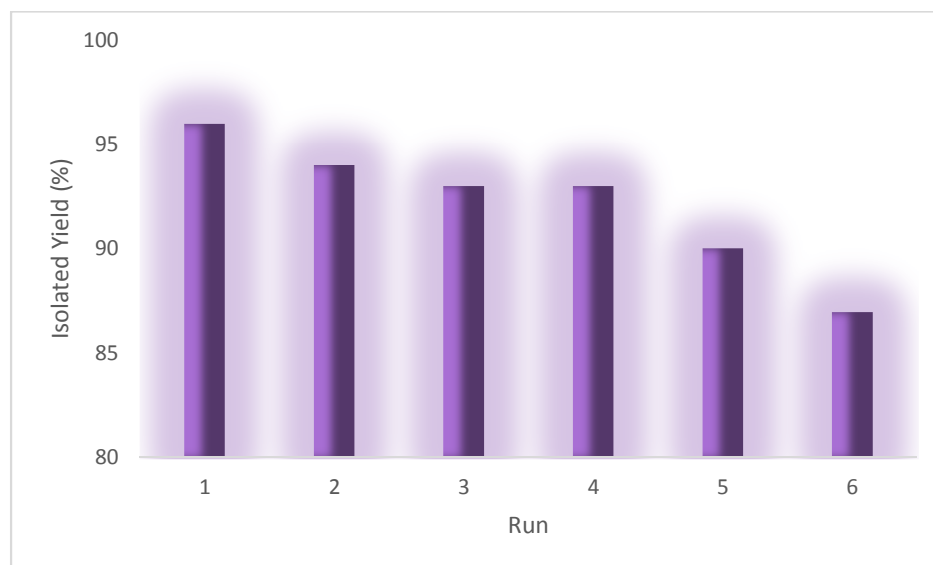


**Fig. 8.** Study of reusability with the Eu@MNPs nanocatalyst.

### 3.4 Exclusivity of the catalytic results:

In order to show the usefulness of Eu@MNPs catalyst, it was compared with other potentially feasible reported heterogeneous catalysts towards the synthesis of a particular tetrahydrobenzo[*b*]pyran derivative (2a) and the results have been documented in table 3. Evidently, in terms of yield, reaction time and reaction conditions, our protocol is superior to the shown catalytic results.

**Table 3.** Comparison of catalytic performance of Eu@MNPs catalyst with that other recently studied catalysts

Sl no.	Reaction conditions	Time (min)	Yield %	Ref.
1	Fe <sub>3</sub> O <sub>4</sub> @SiO <sub>2</sub> @5-SA, 0.02 g, H <sub>2</sub> O, 60 °C	100	92	51
2	TMDPS, ball mill, solvent free, 5 mol%, RT	30	96	52
3	Fe <sub>3</sub> O <sub>4</sub> @g-C <sub>3</sub> N <sub>4</sub> , 0.02 g, EtOH, 60 °C	60	95	53

4	Fe <sub>3</sub> O <sub>4</sub> @THAM@PhSO <sub>3</sub> H, 0.01 g, EtOH/H <sub>2</sub> O, 100 °C	15	90	54
5	[MPim][HSO <sub>4</sub> ]@SBA15, 2 mol %, H <sub>2</sub> O, 45 °C	120	90	55
6	γ-Fe <sub>2</sub> O <sub>3</sub> DMNP, 10 mol%, H <sub>2</sub> O, RT	300	90	56
7	NH <sub>4</sub> H <sub>2</sub> PO <sub>4</sub> /Al <sub>2</sub> O <sub>3</sub> , 0.03 g, EtOH, 78 °C	15	92	57
8	Fe <sub>3</sub> O <sub>4</sub> @SiO <sub>2</sub> /DABCO, 0.05 g, H <sub>2</sub> O, 80 °C	25	90	58
9	MMWCNTs-D-(CH <sub>2</sub> ) <sub>4</sub> SO <sub>3</sub> H, 0.04 g, EtOH, 78 °C	12	98	59
10	GO-Si-NH <sub>2</sub> -PMo, 0.02 g, solvent free, 90 °C	3	97	60
11	TiO <sub>2</sub> /H <sub>2</sub> SO <sub>4</sub> , EtOH, US, 40 °C	15	94	61
12	Fe <sub>3</sub> O <sub>4</sub> @D-NH <sub>2</sub> -HPA, 0.02 g, EtOH, 78 °C	5	91	62
13	Eu@MNPs, 0.03 g, EtOH, RT	25	96	This work

#### 4. Conclusion

In conclusion, we report herein the facile synthesis of the rare earth Eu(III) immobilized over a tetradentate ligand iminodiacetic acid (IDA) functionalized silica modified magnetic CoFe<sub>2</sub>O<sub>4</sub> nanocomposite for the first time. The catalyst was then explored towards the convenient and mild synthesis of diverse range of tetrahydrobenzo[*b*]pyran derivatives under simply stirring in ethanol at room temperature. The catalyst was so efficient that excellent yields were obtained in short reaction times in all the reactions irrespective of nature of substitutions of the substrates. Due to strong magnetic core, the catalyst was easily recovered and reused in six consecutive cycles without a significant loss in catalytic activity.

#### Acknowledgements

The authors are deeply grateful to Iran National Science Foundation (INSF) for financial support (Code number 97009059) and Iran University of Science and Technology for partial support of this research project. BK thanks Gobardanga Hindu College for affiliation.

## References

1. D. Yadav, S. K. Awasthi, *New J. Chem.* 44 (2020) 1320-1325.
2. D. Yadav, S. K. Awasthi, *Dalton Trans.* 49 (2020) 179-186.
3. Subodh, K. Prakash, D. T. Masram, *Dalton Trans.* 49 (2020) 1007-1010.
4. T. Tamoradi, A. Ghorbani-Choghamarani, M. Ghadermazi, *New J. Chem.* 41 (2017) 11714-11721.
5. T. Tamoradi, H. Veisi, B. Karmakar, J. Gholami, *Mater. Sci. Eng. C*, 107 (2020) 110260-110270.
6. Subodh, N. K. Mogha, K. Chaudhary, G. Kumar, D. T. Masram, *ACS Omega*, 3 (2018) 16377-16385
7. F. Sadri, A. Ramazani, A. Massoudi, M. Khoobi, V. Azizkhani, R. Tarasi, L. Dolatyari, B.-K. Min, *B. Korean. Chem. Soc.* 35 (2014) 2029-2032.
8. S. J. Hoseini, V. Heidari, H. Nasrabadi, *J. Mol. Catal. A Chem.* 396 (2015) 90-95.
9. K. Azizi, M. Karimi, A. Heydari, *Tetrahedron Lett.* 56 (2015) 812-816.
10. P. Heidari, R. Cheraghali, H. Veisi, *Appl. Organometal. Chem.* 30 (2016) 991-997.
11. D. Toulemon, B. P. Pichon, X. Cattoën, M. W. C. Man, S. Begin-Colin, *Chem. Commun.* 47 (2011) 11954-11956.
12. M. Arruebo, R. Fernández-Pacheco, M. R. Ibarra, J. Santamaría, *NanoToday* 2(2007) 22-32.
13. H. Teymourian, A. Salimi, S. Khezrian, *BiosensBioelectron* 49 (2013) 1-8.
14. T. Tamoradi, A. Ghorbani-Choghamarani, M. Ghadermazi, *Solid State Sci.* 88 (2019) 81-94.
15. X.-H. Huang, Z.-H. Chen, *Scr. Mater.* 54 (2006) 169-173.
16. K. Chaudhary, Subodh, K. Prakash, N. K. Mogha, D. T. Masram, *Arabian J. Chem.* 13 (2019) 4869-4881.
17. W. S. Shehab, A. A. Ghoneim, *Arab. J. Chem.* 9 (2016) S966-S970.

18. A. M. Dar, S. Uzzaman, *Eur. Chem. Bull.*4 (2015) 249-259.
19. B. Maleki, S. Sheikh, *Org. Prep. Proced. Int.*47 (2015) 368-378.
20. M. G. Dekamin, S. Z. Peyman, Z. Karimi, S. Javanshir, M. R. Naimi-Jamal, M. Barikani, *Int.J.Biol.Macromol.*87 (2016) 172-179.
21. A. R. Saundane, K. Vijaykumar, A. V. Vaijinath, *Bioorg. Med.Chem.Lett.*23 (2013) 1978-1984.
22. A. Hasaninejad, N. Golzar, M. Shekouhy, A. Zare, *Helv. Chim. Acta*94 (2011) 2289-2294.
23. H. A. Oskooie, M. M. Heravi, N. Karimi, M. E. Zadeh, *Synth. Commun.*41 (2011) 436-440.
24. Z. Ye, R. Xu, X. Shao, X. Xu, Z. Li, *Tetrahedron Lett.*51 (2010) 4991-4994.
25. S. Tabassum, S. Govindaraju, M. A. Pasha, *Ultrason.Sonochem.*24 (2015) 1-7.
26. R. Mohammadi, S. Esmati, M. Gholamhosseini-Nazari, R. Teimuri-Mofrad, *J. Mol. Liq.*275 (2019) 523-534.
27. M. G. Dekamin, M. Eslami, *Green Chem.*16 (2014) 4914-4921.
28. H. Sharma, S. Srivastava, *RSC Adv.*8 (2018) 38974-38979.
29. Subodh, K. Chaudhary, K. Prakash, D. T. Masram, *Appl. Surf. Sci.* 509 (2020) 144902-144911
30. Subodh, K. Prakash, K. Chaudhary, D. T. Masram, *Appl. Catal. A-General*, 593 (2020) 117411-117417
31. P. Mohammadi, H. Sheibani, *Mater. Chem. Phys.*228 (2019) 140-146.
32. B. Paplall, S. Nagaraju, P. Veerabhadraiah, K. Sujatha, S. Kanvah, B. V. Kumar, D. Kashinath, *RSC Adv.*4 (2014) 54168-54174.
33. A. Javid, F. Moeinpour, *B. Chem. Soc. Ethiopia*32 (2018) 501-511.
34. M. Bakherad, A. Keivanloo, E. Moradian, A. H. Amin, R. Doosti, M. Armaghan, *J. Iran. Chem. Soc.*15 (2018) 2811-2819.
35. S. S. Katkar, M. K. Lande, B. R. Arbad, S. T. Gaikwad, *Chin. J. Chem.*29 (2011) 199-202.
36. E. Soleimani, M. M. Khodaei, A. T. K. Koshvandi, *Chin. Chem. Lett.*22 (2011) 927-930.
37. E. Soleimani, M. M. Khodaei, A. T. K. Koshvandi, *Synth. Commun.*42 (2012) 1367-1371.

38. E. Soleimani, M. M. Khodaei, A. T. K. Koshvandi, C. R. Chim. 15 (2012) 273-277.
39. A. T. Kal-Kashvandi, M. M. Heravi, S. Ahmadi, T. Hosseinnejad, J. Inorg. Organomet. Polym. Mater. 28 (2018) 1457-1467.
40. A. Maleki, R. Ghalavand, R. Firouzi Haji, Appl. Organometal. Chem. 32 (2018) e3916.
41. R. Mozafari, F. Heidarizadeh, Polyhedron 162 (2019) 263-276.
42. M. Haghghat, F. Shirini, M. Golshekan, J. Nanosci. Nanotechnol. 19 (2019) 3447-3458.
43. T. R. Garbe, M. Kobayashi, N. Shimizu, N. Takesue, M. Ozawa, H. Yukawa, J. Nat. Prod. 63 (2000) 596-598.
44. M. Hajjami, F. Gholamian, R. H. Hudson, A. M. Sanati, Catal. Lett. 149 (2019) 228-247.
45. B. Maleki, M. Baghayeri, S. A. J. Abadi, R. Tayebee, A. Khojastehnezhad, RSC Adv. 6 (2016) 96644-96661.
46. M. A. Zolfigol, M. Safaiee, N. Bahrami-Nejad, New J. Chem. 40 (2016) 5071-5079.
47. D. Azarifar, Y. Abbasi, Synth. Commun. 46 (2016) 745-758.
48. M. Wanzheng, A. G. Ebadi, R. Javahershenas, G. Jimenez, RSC Adv. 9 (2019) 12801-12812.
49. M. Esmaeilpour, J. Javidi, F. Dehghani, F. N. Dodeji, RSC Adv. 5 (2015) 26625-26633.
50. H. Alinezhad, M. Tarahomi, B. Maleki, A. Amiri, Appl. Organometal. Chem. 33 (2019) e4661.
51. F. Saboury, N. Azizi, Z. Mirjafari, M. M. Hashemi, J. Iran. Chem. Soc. (2020) <https://doi.org/10.1007/s13738-020-01948-5>
52. N. G. Khaligh, T. Mihankhah, Mohd R. Johan, J. Mol. Liq. 277 (2019) 794-804
53. N. Azizi, T. S. Ahoovie, M. M. Hashemi, I. Yavari, Synlett, 29 (2018) 645-649
54. H. F. Niya, N. Hazeri, M. R. Kahkhaiye, M. T. Maghsoodlou, Res. Chem. Intermed. (2019) <https://doi.org/10.1007/s11164-019-04056-z>
55. S. Rostamnia, A. Hassankhani, H. Hossieni, H. Golchin, G. Behnam, H. Xin, J. Mol. Catal. A Chem. 395 (2014) 463-469
56. S. Rostamnia, A. Nuri, H. Xin, A. Pourjavadi, S. H. Hosseini, Tetrahedron Lett. 54 (2013) 3344-3347
57. B. Maleki, S. S. Ashrafi, RSC Adv. 4 (2014) 42873-42891.
58. J. Davarpanah, A. R. Kiasat, S. Noorizadeh, M. Ghahremani, J. Mol. Catal. A-Chem. 376 (2013) 78-89

59. F. Adibian, A.R. Pourali, B. Maleki, M. Baghayeri, A. Amiri, *Polyhedron* 175 (2019) 114179-114200
60. F. Ataie, A. Davoodnia, A. Khojastehnezhad, *Polycycl. Aromat. Compd.* (2019) <https://doi.org/10.1080/10406638.2019.1622137>
61. D. Azarifar, S. -M. Khatami, M. A. Zolfigol, R. Nejat-Yami, *J. Iran. Chem. Soc.* 11 (2013) 1223-1230
62. A. Jamshidi, B. Maleki, F. M. Zonoz, R. Tayebbe, *Mater. Chem. Phys.* 209 (2018) 46-59

## Highlights

- Europium (Eu) anchored iminodiacetic acid functionalized silica modified core-shell CoFe<sub>2</sub>O<sub>4</sub> magnetic nanoparticles is produced.
- For the first time, utilization of Europium (Eu) to the preparation of heterogeneous catalysts and the biologically and pharmaceutically organic compounds is developed.
- It was characterized by FT-IR, SEM, EDX, and XRD analyses.
- It was successfully performed for the synthesis of diverse substituted tetrahydrobenzo [b] prawns in green conditions.
- It can be easily recovered by an external magnet and reused six times.

**Declaration of interests**

The authors declare that they have no known competing financial interests or personal relationships that could have appeared to influence the work reported in this paper.

The authors declare the following financial interests/personal relationships which may be considered as potential competing interests:

The authors declare that they have no conflict of interest

Journal Pre-proof